2.3. METHANE

2.3.1. IN SITU METHANE MEASUREMENTS

Quasi-continuous measurements of atmospheric methane continued at MLO and BRW at a frequency of four ambient measurements each hour. The relative precision is 0.07%. Details of the measurement techniques and analysis of the in situ data through early 1994 were published in 1995 [*Dlugokencky et al*., 1995]. Daily averaged methane mole fractions (in 10^{-9} mol mol^{-1}, nmol mol^{-1}) are plotted in Figure 2.11 for BRW (a) and MLO (b). The data were edited for instrument malfunction using a rule-based expert system [*Masarie et al.*, 1991], and they were selected for meteorological conditions. Briefly, the BRW data are constrained to the clean air sector that includes wind direction of 020-110° and wind speed greater than 1 m s^{-1}. MLO data are constrained to periods typically with downslope winds that correspond to 0000-0659 local time.

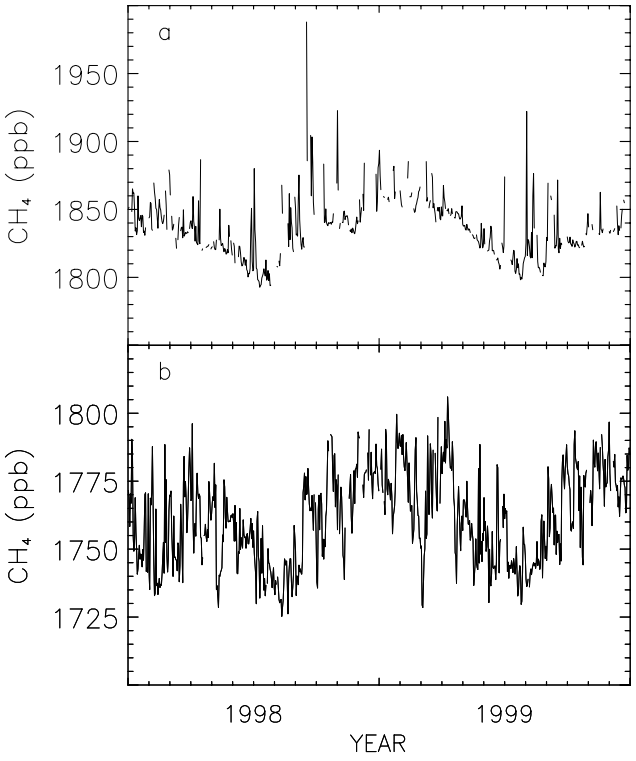

Fig. 2.11. Daily mean CH_4 mixing ratios for (a) Barrow and (b) Mauna Loa for 1998 and 1999. The data are constrained for wind regime, and they have undergone a quality control step to ensure that the analytical instrument was working optimally when they were obtained [*Masarie et al*., 1991].

2.3.2. MEASUREMENTS OF METHANE IN DISCRETE SAMPLES

During 1998-1999 the determination of the global distribution of atmospheric methane continued from 48 sampling sites of the global cooperative air sampling network. Provisional annual mean values for 1998-1999 are given in Table 2.8. Some sites that began prior to 1998 and now have longer, more complete records have been added to Table 2.8. These sites are Assekrem, Algeria (ASK); Christmas Island, Kiribati (CHR); Bobabeb, Namibia (NMB); Plateau Assy, Kazakstan (KZD); and Sary Taukum, Kazakstan (KZM).

During 1998 an interesting anomaly was observed in the CH_4 growth rate, particularly at mid- to high-latitudes in the northern hemisphere. In Figure 2.12 preliminary CH_4 mole fractions for the high northern hemisphere (HNH) are plotted for 1984-1999 in panel a, and the instantaneous deseasonalized and smoothed growth rate is plotted in panel b. Though the increased growth rate in 1998 is unmistakable in Figure 2.12b, a better appreciation of the magnitude of the anomaly may be achieved from Figure 2.12c. In that panel, residuals from a function fitted to the zonal means are plotted as a function of time. The function consists of a second-order polynomial and four harmonic terms. It is reasonable to think of this function as a model of methane's average behavior in the atmosphere where the polynomial represents the long-term average trend and the harmonics represent the average seasonal cycle. This "model" is consistent with the previous suggestion that atmospheric CH_4 is approaching steady state [*Dlugokencky et al*., 1998]. The residuals plotted in Figure 2.12c represent deviations from this model, and they are the result of perturbations to the "average" balance of CH_4 sources and sinks.

Evident in the residuals is noise with three cycles yr^{-1} and an amplitude varying from 4 to 15 ppb. During 1984-1992 the residuals trended upwards, but in 1992 there was a dramatic drop in the residuals followed by a decreasing trend through 1997. *Dlugokencky et al*. [1995] suggested that the decreased growth rate in 1992 could not be explained entirely by decreased emissions from natural wetlands and that perhaps decreased emissions from the fossil fuel sector in the former Soviet Union (FSU), coincident with the collapse of that economy, resulted in the observed change in growth rate. Although the following is quite speculative, one might expect that if decreased emissions from wetlands was the only cause of the observed anomaly in growth rate in 1992, the upward trend in the residuals should have resumed after the wetland emissions recovered. The fact that it did not may suggest that emissions from the fossil sector in the FSU did contribute to the observed anomaly, and that continuing efforts to halt leaks in the natural gas pipelines of the FSU may have prevented a return to emission levels prior to 1992 for this latitude zone. Evidence for this scenario comes from two recent studies of CH_4 emissions from Russia. *Reshetnikov et al.* [2000] estimated 24-40 Tg yr^{-1} CH_4 emissions from the Russian gas industry during the late-1980s and early-1990s. *Dedikov et al.* [1999], using measurements from an extensive program in 1996 and 1997 to determine losses from Russian gas production and transmission facilities, estimated that 3.6 Tg yr^{-1} CH_4 were emitted during that time. The dramatic decrease in emissions suggested by these studies is not supported by our measurements, but decreased production and improved efforts to prevent leaks likely did lead to lower emissions.

TABLE 2.8. Provisional 1998 and 1999 Annual Mean CH_4 Mixing Ratios From the Air Sampling Network

Site Code	Location	1998 CH_4 (ppb)	1999 CH_4 (ppb)
ALT	Alert, N.W.T., Canada	1825.3	1831.7
ASC	Ascension Island	1707.7	1714.8
ASK	Assekrem, Algeria	1770.4	1779.7
AZR	Terceira Island, Azores	1796.8	1805.2
BAL	Baltic Sea	1850.7	1858.8
BME	Bermuda (east coast)	1799.3	1799.4
BMW	Bermuda (west coast)	1789.1	1795.8
BRW	Barrow, Alaska	1836.7	1841.0
BSC	Black Sea, Constanta, Romania	1919.4	1936.9
CBA	Cold Bay, Alaska	1823.5	1826.5
CGO	Cape Grim, Tasmania	1695.3	1705.7
CHR	Christmas Island, Kiribati	[ ]	1736.0
CRZ	Crozet Island	1694.6	[ ]
EIC	Easter Island, Chile	1695.8	1705.7
GMI	Guam, Mariana Islands	1754.1	1753.9
GOZ	Gozo Island, Malta	[ ]	[ ]
HBA	Halley Bay, Antarctica	1694.7	1704.8
HUN	Hegyhatsal, Hungary	1887.5	1893.2
ICE	Vestmanaeyjar, Iceland	1826.9	1827.2
ITN	WITN, Grifton, North Carolina	1853.8	[ ]
IZO	Izana Obs., Tenerife	1778.8	1782.1
KCO	Kaashidhoo, Maldives	1743.0	[ ]
KEY	Key Biscayne, Florida	1788.8	1796.8
KUM	Cape Kumukahi, Hawaii	1777.5	1778.8
KZD	Plateau Assy, Kazakstan	1844.0	1845.6
KZM	Sary Taukum, Kazakstan	1808.4	1812.2
LEF	WLEF, Park Falls, Wisconsin	1841.4	1859.6
MHD	Mace Head, Ireland	1811.7	1822.4
MID	Midway Island	1786.7	1784.2
MLO	Mauna Loa, Hawaii	1755.9	1764.2
NMB	Bobabeb, Namibia	[ ]	1715.3
NWR	Niwot Ridge, Colorado	1787.2	1793.7
PSA	Palmer Station, Antarctica	1694.9	1705.5
PTA	Point Arena, California	[ ]	1822.1
RPB	Ragged Point, Barbados	1758.3	1767.7
SEY	Mahe Island, Seychelles	1717.5	1724.4
SHM	Shemya Island, Alaska	1822.8	1825.3
SMO	American Samoa	1697.8	1713.7
SPO	South Pole, Antarctica	1694.1	1704.7
STM	Ocean Station M	1823.6	1828.2
SYO	Syowa Station, Antarctica	1694.3	1704.7
TAP	Tae-ahn Peninsula, South Korea	1851.8	1859.5
TDF	Tierra Del Fuego, Argentina	1694.7	1706.2
UTA	Wendover, Utah	1799.9	1808.4
UUM	Ulaan Uul, Mongolia	1821.6	1825.8
WIS	Sede Boker, Negev Desert, Israel	1825.6	1828.9
WLG	Mt. Waliguan, China	1790.1	1802.4
ZEP	Ny-Alesund, Svalbard	1830.3	1832.7

Note: square brackets indicate insufficient data to calculate the annual mean.

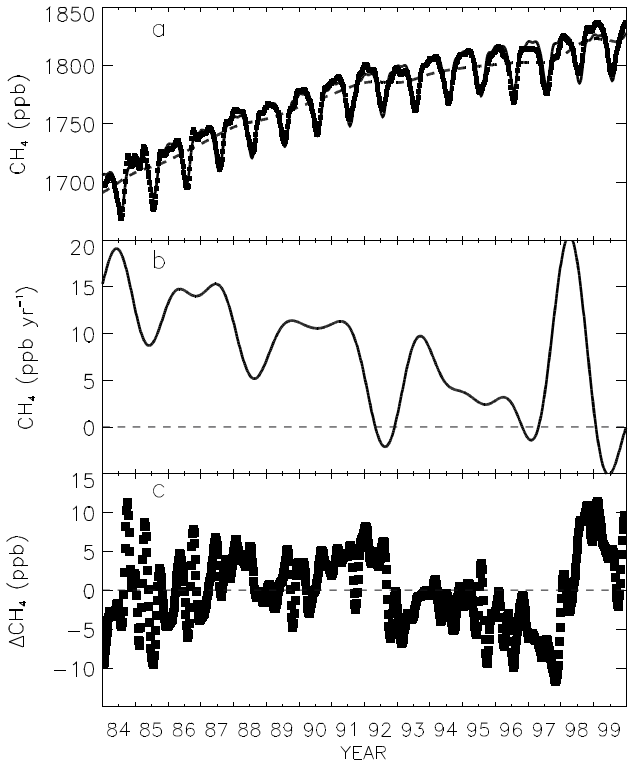

Fig. 2.12. (a) Methane mole fractions for the high northern latitudes (30-90ºN; HNH). The solid line is a function (2nd-order polynomial + 4 harmonics) fitted to the zonal means. The dashed line is a deseasonalized trend fitted to the zonal means. (b) Instantaneous CH_4 growth rate for HNH. It is calculated as the derivative of the dashed curve in 2.12a; (c) Residuals from function (solid line in 2.12a) fitted to HNH zonal averages.

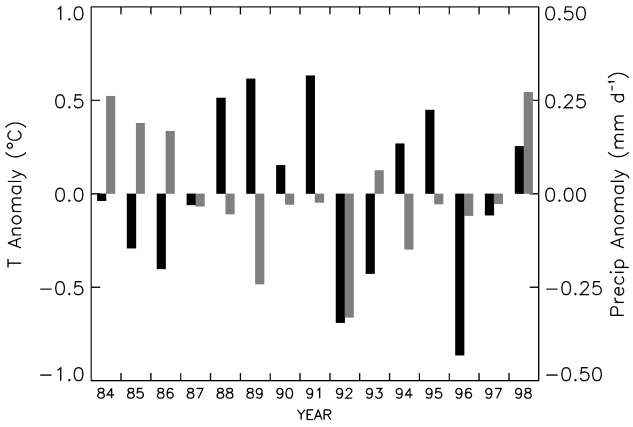

Fig. 2.13. Temperature (black) and precipitation (gray) anomalies for northern wetland regions during 1984-1998.

In 1998 there was a large positive anomaly in the residuals that shows signs of recovering at the end of 1999. Since natural wetlands are an important source of CH_4 in this latitude zone, changes in their emissions are always a possibility when an anomalous CH_4 growth rate is observed. The two most sensitive parameters for CH_4 emissions from wetlands are soil temperature and soil moisture. In Figure 2.13 air temperature (T) and precipitation anomalies are plotted for inundated wetland regions only; these are used as a proxy for the soil parameters. There are clear positive T and precipitation anomalies in 1998. Noteworthy are the negative T and precipitation anomalies in 1992. Using a process-model, large (10 Tg) anomalies were calculated in wetland CH_4 emissions for these 2 years, negative in 1992 and positive in 1998 (B. Walter, Columbia University, private communication, 2000). Although uncertainties on these estimates are large, they implicate wetlands as a contributor to both anomalies observed in CH_4 growth rates. Additionally, there were large boreal forest fires in North America and Siberia during 1998 that potentially contributed to the CH_4 growth rate

anomaly (E. Kasischke, University of Maryland, private communication, 2000). Estimates of emissions from these fires are ongoing (see section 2.4.1).

2.3.3. MEASUREMENT OF $^{13}C/^{12}C$ OF METHANE BY MASS SPECTROMETRY

Partitioning atmospheric methane into its bacterial, thermal, and biomass burning sources is possible through global measurements of its stable carbon isotopic ratio $^{13}C/^{12}C$. Ratios are expressed in permil (a one part per thousand relative deviation from a standard isotopic ratio). Biological sources, such as wetlands, have a characteristic isotopic composition (typically -60‰) that is more depleted in the heavy isotope, ^{13}C, than thermal sources like natural gas (-40‰), which, in turn, are more depleted than the biomass burning source (-25‰). The measured isotopic ratio of atmospheric methane (-47‰) is a composite of these sources, but it is also influenced by the enrichment in ^{13}C content (+5‰) that results from the destruction of methane by the hydroxyl radical, which is slightly more rapid for $^{12}CH_4$ than for $^{13}CH_4$.

An automated system was designed for the analysis of ^{13}C in atmospheric methane. Starting in January 1998 the system has analyzed pairs of flasks, on a weekly basis, from six sites (SPO, Cape Grim Tasmania (CGO), SMO, MLO, NWR, and BRW) of the global cooperative air sampling network. From a sampling flask, 200 mL of air is used to achieve a precision of better than 0.06‰ in less than 15 minutes. The measured precision is comparable to that of systems where at least 100 times as much air is used and where the analysis takes more than 1 hour. Starting in June 1998 an automated flask manifold was introduced that allows for a greater throughput of samples than would otherwise be possible. The CMDL standard scale is now linked to a scale maintained by the University of California, Irvine (UCI). In the summer of 2000 a program that includes both CMDL and the UCI laboratories will measure $^{13}CH_4$ in small cylinders collected at NWR.

Measurements indicate an annual average latitudinal difference of approximately -0.5‰ (BRW-SPO) (Figure 2.14). The sign of this gradient is explained by the predominance of methane sources, which are generally depleted relative to the atmospheric average, in the northern hemisphere, whereas the dominant methane sink, OH, is more evenly distributed. The magnitude of the gradient and how it changes seasonally are a result of changing OH and source emission patterns.

Distinct seasonal variations are also evident at each of the six sites. At the northern hemisphere sites of BRW and NWR seasonal variations appear to be driven by seasonality in source emissions, but the variations at the southern hemisphere sites, CGO and SPO, appear to be driven by OH seasonality (Figure 2.15). At MLO and SMO seasonal variations are less distinct. Curiously the amplitude of the seasonal cycle of $\delta^{13}C$ at CGO (0.3‰) cannot be explained solely by destruction by OH, while the seasonal cycle amplitude of $\delta^{13}C$ at SPO can be. This is especially intriguing in light of the strong similarity in the amplitude of the mole fraction seasonal cycles at the two sites. The analysis of intra-annual variations in $^{13}C/^{12}C$ at individual sites as well as inter-annual variations at all the sites are likely to contribute to a better understanding of methane budgets on continental and global scales.

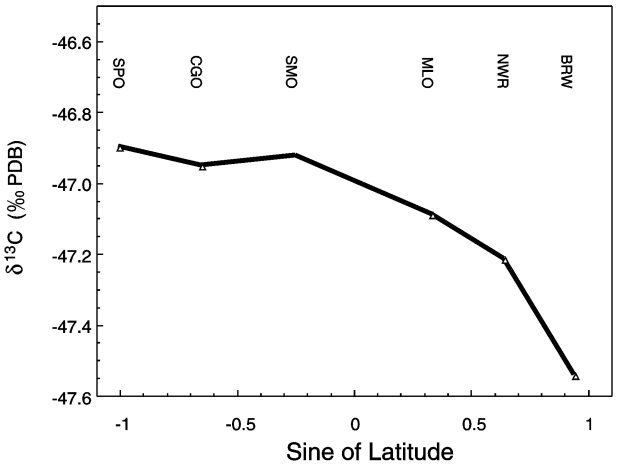

Fig. 2.14. Annual mean latitude gradient of $\delta^{13}C$ of CH_4.

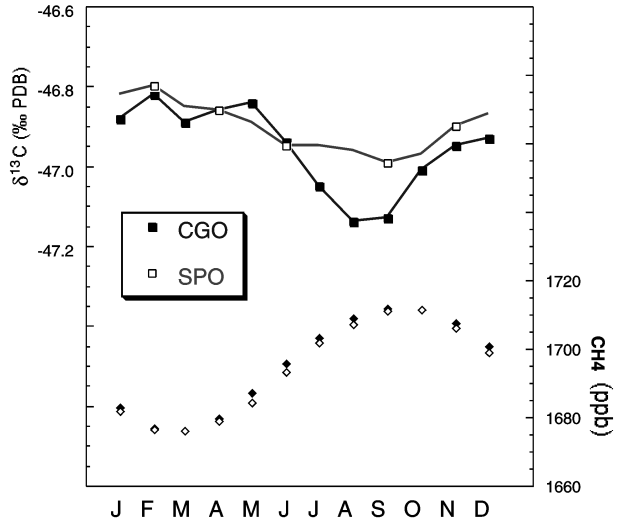

Fig. 2.15. Average seasonal cycle of CH_4 and its $^{13}C/^{12}C$ ratio at Cape Grim (CGO) and at the south pole (SPO).

2.3.4. $^{13}C/^{12}C$ AND D/H ISOTOPIC RATIO ANALYSIS OF METHANE BY INFRARED SPECTROSCOPY

The goal of this methane isotopic measurement program is to develop a robust infrared absorption spectrometer to measure both $^{13}C/^{12}C$ and D/H isotopic ratios in atmospheric methane samples with sufficient sensitivity to resolve spatial and temporal trends. The instrument is being developed in cooperation with the Optical Frequency Measurements Group at the U.S. National Institute of Standards and Technology (NIST), and samples will be obtained from the CCGG global cooperative air sampling network to provide a good spatial distribution of sampling sites

from which to obtain global methane variability data. To date, measurements of atmospheric methane $^{13}C/^{12}C$ and D/H values have been largely regional and performed almost exclusively by isotope ratio mass spectrometry (section 2.3.3) [*Tyler et al.*, 1999; *Wahlen et al.*, 1990].

Since $^{13}CH_4$ and $^{12}CH_3D$ have the same isotopic mass, their separate measurement requires extensive procedures to convert the CH_4 to CO_2 and H_2. Infrared absorption spectroscopy offers a simple, nondestructive way to measure the stable isotopic composition of atmospheric methane samples. A mid-infrared absorption spectrometer was constructed for stable isotope ratio measurements of atmospheric methane. The spectrometer employs periodically poled lithium niobate (PPLN) to generate difference frequency radiation from two near-infrared diode lasers (one at 811 nm and the other at 1066 nm). This technique yields about 10 microwatts of single mode, tunable radiation that probes the ν3 rotational-vibrational absorption band at 3.4 microns. The radiation is passed through a multipass absorption cell with a path length of 36 m and a volume of 0.3 L. Second harmonic wavelength modulation is used to reduce spectrometer noise. The current 3σ detection limit is 2 ppb of methane in 50 torr of air for a noise-equivalent bandwidth of 1 Hz.

Since the tropospheric mixing ratio of $^{12}CH_3D$ is close to 1 ppb and is comparable to the instrument detection limit, a procedure to concentrate methane samples is required before isotopic analysis. Methane is extracted from 25 L of air using a cryogenic chromatographic column and is injected into the multipass cell with a final total pressure of ~70 torr. This procedure enriches the methane samples by ~1000 times. The abundance of the rare isotopic species ($^{13}CH_4$ and $^{12}CH_3D$) are measured relative to $^{12}CH_4$ by comparing the absorbance of an intrinsically strong spectral line of a rare species with a weak line of $^{12}CH_4$. Thus far a precision of 1.7% for the isotope ratios has been attained. The precision is limited by long-term spectral baseline instabilities arising from optical interference fringes in the multipass cell. With spectral baseline subtraction and the addition of a reference absorption cell, the precision is expected to improve by an order of magnitude.